Quantum State Reduction by Matter-Phase-Related Measurements in Optical Lattices

Wojciech Kozlowski[1,*]**, Santiago F. Caballero-Benitez**[1,2]**, and Igor B. Mekhov**[1,3]

[1]Department of Physics, Clarendon Laboratory, University of Oxford, Parks Road, Oxford OX1 3PU, United Kingdom
[2]CONACYT, Instituto Nacional de Astrofísica, Óptica y Electrónica, Calle Luis Enrique Erro No. 1, Sta. María Tonantzintla, Pue. CP 72840, México
[3]St. Petersburg State University, Universitetsky pr. 26,198504 St. Petersburg, Russia
[*]wojciech.kozlowski@physics.ox.ac.uk

ABSTRACT

A many-body atomic system coupled to quantized light is subject to weak measurement. Instead of coupling light to the on-site density, we consider the quantum backaction due to the measurement of matter-phase-related variables such as global phase coherence. We show how this unconventional approach opens up new opportunities to affect system evolution. We demonstrate how this can lead to a new class of final states different from those possible with dissipative state preparation or conventional projective measurements. These states are characterised by a combination of Hamiltonian and measurement properties thus extending the measurement postulate for the case of strong competition with the system's own evolution.

Introduction

Ultracold gases trapped in optical lattices is a very successful and interdisciplinary field of research[1,2]. Whilst normally the atoms are manipulated using classical light beams there is a growing body of work based on coupling such systems to quantised optical fields exploring the ultimate quantum level of light-matter coupling[3,4]. This new regime of interactions has already led to a host of fascinating phenomena, such as novel methods of non-destructive probing of quantum states[5–14], new quantum phases and light-matter entanglement,[15–23], or an entirely new class of many-body dynamics due to measurement backaction[24–31]. Furthermore, recent experimental breakthroughs in coupling an optical lattice to a cavity demonstrate the significant interest in studying this ultimate quantum regime of light-matter interaction[32,33].

Light scatters due to its interaction with the dipole moment of the atoms which for off-resonant light results in an effective coupling with atomic density, not the matter-wave amplitude. Therefore, it is challenging to couple light to the phase of the matter-field, as is typical in quantum optics for optical fields. Most of the existing work on measurement couples directly to atomic density operators[3,11,26,27,34]. However, it has been shown that it is possible to couple to the the relative phase differences between sites in an optical lattice by illuminating the bonds between them[13,20–23,35]. This is a multi-site generalisation of previous double-well schemes[36–40], although the physical mechanism is fundametally different as it involves direct coupling to the interference terms caused by atoms tunnelling rather than combining light scattered from different sources.

Coupling to phase observables in lattices has been proposed and considered in the context of nondestructive probing and quantum optical potentials. In this paper, we go beyond any previous work by studying this new feature of optical lattice cavity systems in the context of measurement backaction. The quantum trajectory approach to backaction induced dynamics is not new in general and has attracted significant experimental interest in single atom cavity[41] and single qubit circuit[42,43] QED systems. However, its study in the context of many-body dynamics is much more recent and has attracted significant theoretical interest over the past years[3,7,24,29,44–48]. Here, it is the novel combination of measurement backaction as the physical mechanism driving the dynamics and phase coherence as the observable, which the optical fields couple to, that provides a completely new opportunity to affect and manipulate the quantum state.

In this paper we begin by presenting a simple quantum gas example. In the second part we generalize our model and show a novel type of a projection due to measurement which occurs even when there is significant competition with the Hamiltonian dynamics. This projection is fundamentally different to dissipative steady states, standard formalism eigenspace projections or the quantum Zeno effect[49–53] thus providing an extension of the measurement postulate to dynamical systems subject to weak measurement. Such a measurement-based preparation is unobtainable using the dissipative state engineering, as the dissipation would completely destroy the coherence in this case.

Results

Quantum gas model

We consider measurement of an ultracold gas of N bosons trapped in an optical lattice with period a and M sites[3]. We focus on the one-dimensional case, but the general concept can be easily applied to higher dimensions. The isolated system is described by the Bose-Hubbard model with the Hamiltonian

$$\hat{H}_0 = -J\sum_m \hat{p}_m + (U/2)\sum_m \hat{n}_m(\hat{n}_m - 1), \tag{1}$$

where $\hat{n}_m = b_m^\dagger b_m$ is the number operator at site m, b_m annihilates an atom at site m, $\hat{p}_m = b_m^\dagger b_{m+1} + b_m b_{m+1}^\dagger$, J is the atom hopping amplitude and U the on-site interaction.

The atoms are illuminated with an off-resonant beam and light scattered at a particular angle is selected and enhanced by a cavity with decay rate κ[54–56]. Just like in classical optics for light amplitude, the Heisenberg annihilation operator of the scattered light is given by $\hat{a} \sim \int u_{\text{out}}^*(\mathbf{r})u_{\text{in}}(\mathbf{r})\hat{n}(\mathbf{r})d\mathbf{r}$, where $\hat{n}(\mathbf{r}) = \hat{\Psi}^\dagger(\mathbf{r})\hat{\Psi}(\mathbf{r})$ is the atomic density operator, $\hat{\Psi}(\mathbf{r})$ is the operator that annihilates a boson at $\mathbf{r}$, and $u_{\text{in,out}}(\mathbf{r})$ are the light mode functions for the incoming and scattered beams. Expanding the matter-field operator in terms of the Wannier functions of the lowest band, $\hat{\Psi}(\mathbf{r}) = \sum_m b_m w(\mathbf{r} - \mathbf{r}_m)$, we can write $\hat{a} = C(\hat{D} + \hat{B})$[3,7], where C is the Rayleigh scattering coefficient and

$$\hat{D} = \sum_m^K J_{m,m}\hat{n}_m, \quad \hat{B} = \sum_m^K J_{m,m+1}\hat{p}_m, \tag{2}$$

the sum is over K illuminated sites, and

$$J_{m,n} = \int w(\mathbf{r} - \mathbf{r}_m)u_{\text{out}}^*(\mathbf{r})u_{\text{in}}(\mathbf{r})w(\mathbf{r} - \mathbf{r}_n)\,d\mathbf{r}. \tag{3}$$

We will consider the case when the quantum potential due to the cavity light field is negligible (cavity detuning must be small compared to κ[20]), but the photons leak from the cavity and thus affect the system via measurement backaction instead[3,29]. This process can be modelled using a quantum trajectory approach where each experimental run is simulated using a stochastic Schrödinger equation. Following the formalism presented in Ref.[29] the system can be shown to evolve according to $\hat{H} = \hat{H}_0 - i\kappa\hat{a}^\dagger\hat{a}$ and the jump operator $\hat{a}$ is applied to the wave function whenever a photon is detected. In a trajectory simulation the photodetection times are determined using a Monte-Carlo method. Measurement backaction affects the optical field which is entangled with the atoms and thus the quantum gas is also affected, just like the particles in the Einstein-Podolsky-Rosen thought experiment are affected by measurements on its pair[57].

In general, it is easier for the light to couple to atom density that is localised within the lattice rather than the density within the bonds, i.e. in between the lattice sites. This means that in most cases $\hat{D} \gg \hat{B}$ and thus $\hat{a} \approx \hat{D}$. However, it is possible to arrange the light geometry in such a way that scattering from the atomic density operators within a lattice site is suppressed leading to a situation where light is only scattered from these bonds leading to an effective coupling to phase-related observables, $\hat{a} = C\hat{B}$[13]. This does not mean that light actually scatters from the matter phase. Light scatters due to its interaction with the dipole moment of the atoms which for off-resonant light and thus the scattering is always proportional to the density distribution. However, in an optical lattice, the interference of matter waves between neighbouring sites leads to density modulations which allows us to indirectly measure these phase observables. A brief summary based on Ref.[13] on how this is achieved is available in the Supplementary Information online. Here, we will summarise the results and focus on the effects of measurement backaction due to such coupling.

If we consider both incoming and outgoing beams to be standing waves, $u_{\text{in,out}} = \cos(k_{\text{in,out}}^x x + \varphi_{\text{in,out}})$ we can suppress the $\hat{D}$-operator contribution by crossing the beams at angles such that x-components of the wavevectors are $k_{\text{in,out}}^x = \pi/d$, and the phase shifts satisfy $\varphi_{\text{in}} + \varphi_{\text{out}} = \pi$ and $\varphi_{\text{in}} - \varphi_{\text{out}} = \arccos[\mathscr{F}[w^2(\mathbf{r})](2\pi/a)/\mathscr{F}[w^2(\mathbf{r})](0)]/2$, where $\mathscr{F}[f(\mathbf{r})]$ denotes a Fourier transform of $f(\mathbf{r})$[13]. For clarity, this arrangement is illustrated in Fig. 1(a). This ensures that $J_{m,m} = 0$ whilst

$$J_1 \equiv J_{m,m+1} = \mathscr{F}[w(\mathbf{r} - \mathbf{a}/2)w(\mathbf{r} + \mathbf{a}/2)](2\pi/a)/2, \tag{4}$$

a constant, and thus $\hat{a} = C\hat{B}_1$ ($\hat{D} = 0$, $\hat{B} = \hat{B}_1$) with

$$\hat{B}_1 = \sum_m^K J_1\hat{p}_m = 2J_1\sum_k c_k^\dagger c_k \cos(ka), \tag{5}$$

where the second equality follows from converting to momentum space via $b_m = \frac{1}{\sqrt{M}}\sum_k e^{-ikma}c_k$ and c_k annihilates an atom with momentum k.
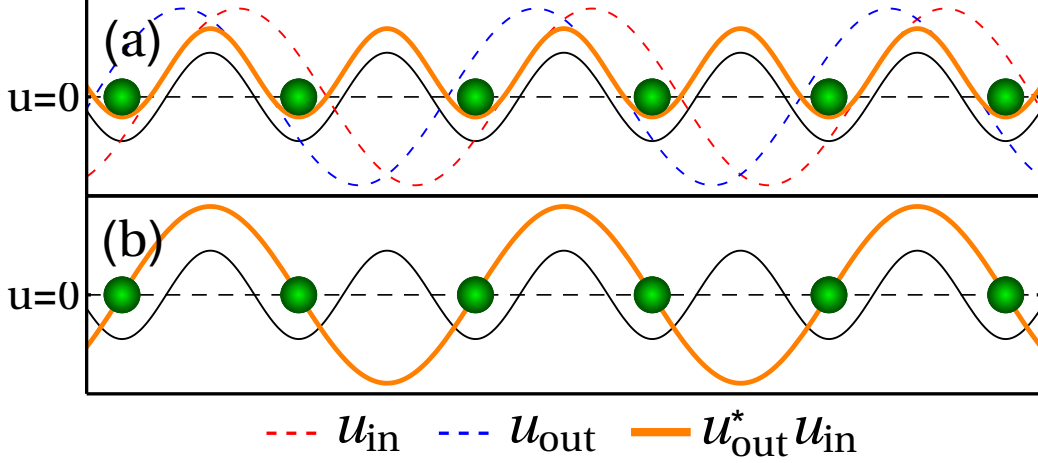
Figure 1. Light field arrangements which maximise coupling, $u_{\text{out}}^* u_{\text{in}}$, between lattice sites. The thin black line indicates the trapping potential (not to scale). (a) Arrangement for the uniform pattern $J_{m,m+1} = J_1$. (b) Arrangement for spatially varying pattern $J_{m,m+1} = (-1)^m J_2$; here $u_{\text{in}} = 1$ so it is not shown and u_{out} is real thus $u_{\text{out}}^* u_{\text{in}} = u_{\text{out}}$.

In order to correctly describe the dynamics of a single quantum trajectory we have introduced a non-Hermitian term to the Hamiltonian, $-i\kappa\hat{a}^\dagger\hat{a}$. As the jump operator itself, $\hat{a}$ is linearly proportional to the atom density, the new term introduces a quadratic atom density term on top of the nonlocality due to the global nature of the probing. Therefore, in order to focus on the competition between tunnelling and measurement backaction we do not consider the other (standard) nonlinearity due to the atomic interactions: $U = 0$. Therefore, $\hat{B}_1$ is proportional to the Hamiltonian and both operators have the same eigenstates, i.e. Fock states in the momentum basis. We can thus rewrite as

$$\hat{H} = -\frac{J}{J_1}\hat{B}_1 - i\kappa|C|^2\hat{B}_1^\dagger\hat{B}_1, \tag{6}$$

which will naturally be diagonal in the $\hat{B}_1$ basis. Since it's already diagonal we can easily solve its dynamics and show that the probability distribution of finding the system in an eigenspace with eigenvalue B_1 after n photocounts at time t is given by

$$p(B_1, n, t) = \frac{B_1^{2n}}{F(t)} \exp\left[-2\kappa|C|^2 B_1^2 t\right] p_0(B_1), \tag{7}$$

where $p_0(B_1)$ denotes the initial probability of observing B_1[7,44,45] and $F(t)$ is the normalisation factor. This distribution has peaks at $B_1 = \pm\sqrt{n/2\kappa|C|^2 t}$ and an initially broad distribution will narrow down around these two peaks with time and successive photocounts. The final state is in a superposition, because we measure the photon number, $\hat{a}^\dagger\hat{a}$ and not field amplitude. Therefore, the measurement is insensitive to the phase of $\hat{a} = C\hat{B}$ and we get a superposition of $\pm B_1$. This means that the matter is still entangled with the light as the two states scatter light with different phase which the photocount detector cannot distinguish. However, this is easily mitigated at the end of the experiment by switching off the probe beam and allowing the cavity to empty out or by measuring the light phase (quadrature) to isolate one of the components[3,7,14]. Interestingly, this measurement will establish phase coherence across the lattice, $\langle b_m^\dagger b_n \rangle \neq 0$, in contrast to density based measurements where the opposite is true, Fock states with no coherences are favoured.

Unusually, we do not have to worry about the timing of the quantum jumps, because the measurement operator commutes with the Hamiltonian. This highlights an important feature of this measurement - it does not compete with atomic tunnelling, and represents a quantum nondemolition (QND) measurement of the phase-related observable[58]. This is in contrast to conventional density based measurements which squeeze the atom number in the illuminated region and thus are in direct competition with the atom dynamics (which spreads the atoms), thus requiring strong couplings for a projection[29]. Here a projection is achieved at any measurement strength which allows for a weaker probe and thus effectively less heating and a longer experimental lifetime.

It is also possible to achieve a more complex spatial pattern of $J_{m,m+1}$[13]. This way the observable will no longer commute with the Hamiltonian (and thus will no longer be QND), but will still couple to the phase related operators. This can be done by tuning the angles such that the wavevectors are $k_{\text{in}}^x = 0$ and $k_{\text{out}}^x = \pi/d$ and the phase shift of the outgoing beam is $\varphi_{\text{out}} = \pm\pi/d$.

This yields

$$(-1)^m J_2 \equiv J_{m,m+1} = -(-1)^m \mathscr{F}[w(\mathbf{r}-\mathbf{a}/2)w(\mathbf{r}+\mathbf{a}/2)](\pi/a)\cos(\varphi_{\text{in}}), \qquad (8)$$

where J_2 is a constant. Now $\hat{a} = C\hat{B}_2$ ($\hat{D} = 0$, $\hat{B} = \hat{B}_2$) and the resulting coupling pattern is shown in Fig. 1(b). The operator $\hat{B}_2$ is given by,

$$\hat{B}_2 = \sum_m^K (-1)^m J_2 \hat{p}_m = 2iJ_2 \sum_k c_k^\dagger c_{k-\pi/a}\sin(ka). \qquad (9)$$

Note how the measurement operator now couples the momentum mode k with the mode $k - \pi/a$.

The measurement operator no longer commutes with the Hamiltonian so we do not expect there to be a steady state as before. In order to understand the measurement it will be easier to work in a basis in which it is diagonal. We perform the transformation $\beta_k = \frac{1}{\sqrt{2}}\left(c_k + ic_{k-\pi/a}\right)$, $\tilde{\beta}_k = \frac{1}{\sqrt{2}}\left(c_k - ic_{k-\pi/a}\right)$, which yields the following forms of the measurement operator and the Hamiltonian:

$$\hat{B}_2 = 2J_2 \sum_{\text{RBZ}} \sin(ka)\left(\beta_k^\dagger \beta_k - \tilde{\beta}_k^\dagger \tilde{\beta}_k\right), \qquad (10)$$

$$\hat{H}_0 = 2J \sum_{\text{RBZ}} \cos(ka)\left(\beta_k^\dagger \tilde{\beta}_k + \tilde{\beta}_k^\dagger \beta_k\right), \qquad (11)$$

where the summations are performed over the reduced Brilluoin Zone (RBZ), $0 < k \leq \pi/a$, to ensure the transformation is canonical. We see that the measurement operator now consists of two types of modes, β_k and $\tilde{\beta}_k$, which are superpositions of two momentum states, k and $k - \pi/a$. Note how a spatial pattern with a period of two sites leads to a basis with two modes whilst a uniform pattern had only one mode, c_k.

Trajectory simulations confirm that there is no steady state. However, unexpectedly, for each trajectory we observe that the dynamics always ends up confined to some subspace as seen in Fig. 2 which is not the same for each trajectory. In general, this subspace is not an eigenspace of the measurement operator or the Hamiltonian. In Fig. 2(b) it in fact clearly consists of multiple measurement eigenspaces. This clearly distinguishes it from the typical projection formalism. It is also not the quantum Zeno effect which predicts that strong measurement can confine the evolution of a system as this subspace must be an eigenspace of the measurement operator[49–53]. Furthermore, the projection we see in Fig. 2 occurs for even weak measurement strengths compared to the Hamiltonian's own evolution, a regime in which the quantum Zeno effect does not happen. It is also possible to dissipatively prepare quantum states in an eigenstate of a Hamiltonian provided it is also a dark state of the jump operator, $\hat{a}|\Psi\rangle = 0$,[59]. However, this is also clearly not the case here as the final state in Fig. 2(c) is not only not confined to a single measurement operator eigenspace, it also spans multiple Hamiltonian eigenspaces. Therefore, the dynamics induced by $\hat{a} = C\hat{B}_2$ projects the system into some subspace, but since this does not happen via any of the mechanisms described above it is not immediately obvious what this subspace is.

A crucial point is that whilst single quantum trajectories might not have a steady state, for dissipative systems the density matrix will in general have a steady state which can undergo phase transitions as the dissipative parameters are varied[60]. If we were to average over many trajectories we would obtain such a steady state for this system. However, we are concerned with measurement and not dissipation. Whilst both are open systems, having knowledge of the measurement outcome from the photodetector means we deal with pure states that are the outcomes of individual measurements rather than an ensemble average over all possible outcomes. This can reveal physical effects which would be lost in a mixed state. The example in Fig. 2 shows how a single quantum trajectory can become confined yet never approach any steady state - measurement and tunnelling still compete, albeit in a limited subspace. This subspace will not in general be the same for each experimental trajectory, but once the subspace is chosen, the system will remain there. This is analogous to a QND measurement in which a system after the first projection will remain in its chosen eigenstate, but this eigenstate is not determined until the first projection takes place. However, if we were to look at the dissipative steady state (by averaging expectation values over many quantum trajectories), we would not see these subspaces at all, because the mixed state is an average over all possible outcomes, and thus an average over all possible subspaces which on a single trajectory level are mutually exclusive. Therefore, here we will consider only individual experimental runs, which are not steady states themselves, but rather the individual pure state components of the dissipative steady state that are obtained via the weak measurement of $\hat{B}_2$.

General model for the projection

To understand this dynamics we will look at the master equation for open systems described by the density matrix, $\hat{\rho}$,

$$\dot{\hat{\rho}} = -i\left[\hat{H}_0, \hat{\rho}\right] + 2\kappa\left[\hat{a}\hat{\rho}\hat{a}^\dagger - \frac{1}{2}\left(\hat{a}^\dagger \hat{a}\hat{\rho} + \hat{\rho}\hat{a}^\dagger \hat{a}\right)\right], \qquad (12)$$
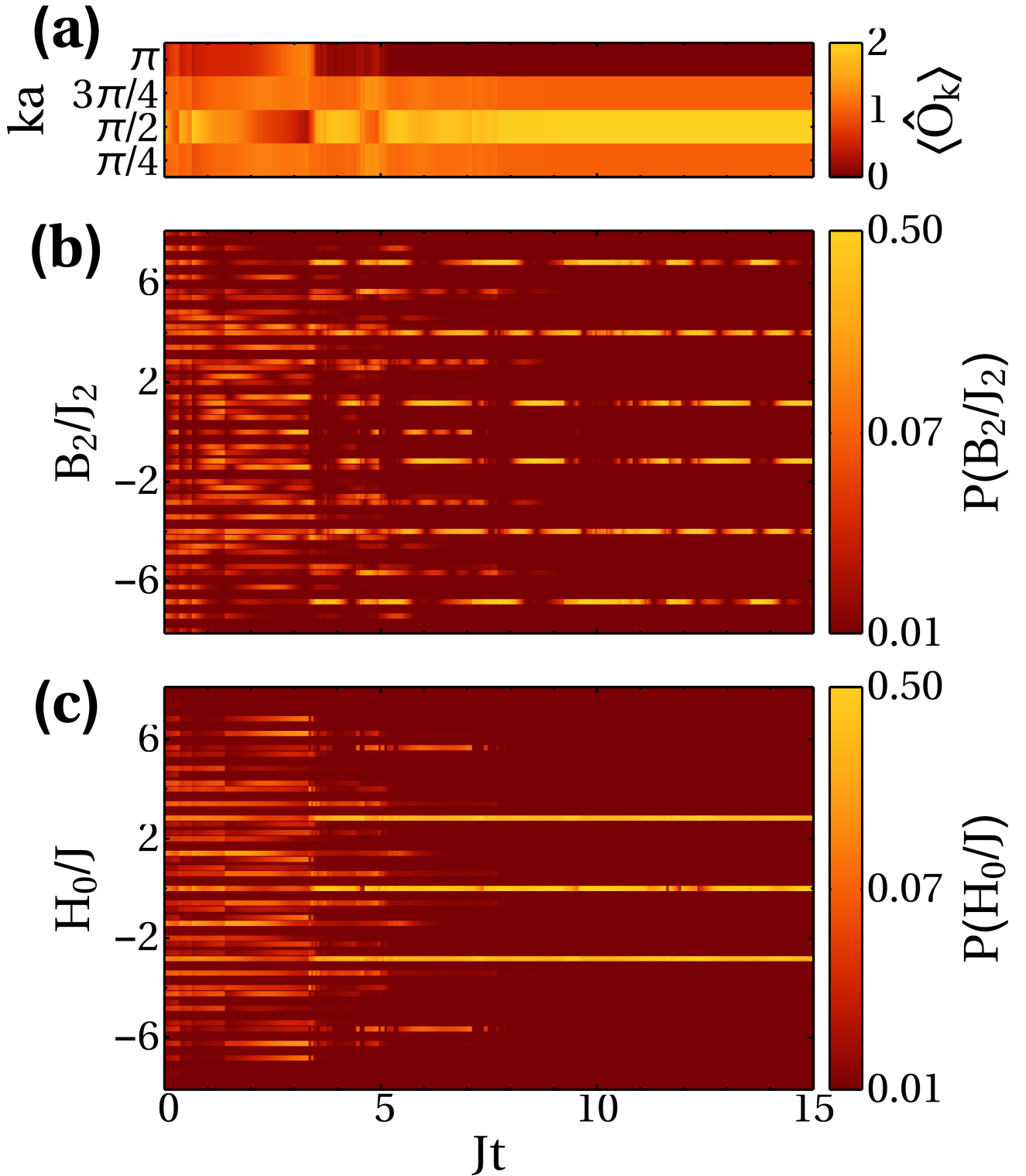
Figure 2. Subspace projections. Projection to a $\mathscr{P}_M$ space for four atoms on eight sites with periodic boundary conditions. The parameters used are $J = 1$, $U = 0$, $\kappa|C|^2 = 0.1$, and the initial state was $|0,0,1,1,1,1,0,0\rangle$. (a) The $\langle\hat{O}_k\rangle = \langle\hat{n}_k + \hat{n}_{k-\pi/a}\rangle$ distribution becomes fully confined to its subspace at $Jt \approx 8$ indicating the system has been projected. (b) Populations of the $\hat{B}_2$ eigenspaces. (c) Population of the $\hat{H}_0$ eigenspaces. Once the projection is achieved at $Jt \approx 8$ we can see from (b-c) that the system is not in an eigenspace of either $\hat{B}_2$ or $\hat{H}_0$, but it becomes confined to some subspace. The system has been projected onto a subspace, but it is neither that of the measurement operator or the Hamiltonian.

where $\hat{a} = C(\hat{D} + \hat{B})$ as before. This equation describes the state of the system if we discard all knowledge of the outcome which is effectively an average over all possible stochastic quantum trajectories. The commutator describes coherent dynamics due to the isolated Hamiltonian and the remaining terms are due to measurement. This is a convenient way to find features of the dynamics common to every measurement trajectory.

We define the projectors of the measurement eigenspaces, P_m, which have no effect on any of the (possibly degenerate) eigenstates of $\hat{a}$ with eigenvalue a_m, but annihilate everything else, thus $P_m = \sum_{a_n=a_m} |a_n\rangle\langle a_n|$, where $|a_n\rangle$ is an eigenstate of $\hat{a}$ with eigenvalue a_n. Note that since $\hat{a} = C(\hat{D} + \hat{B})$ these projectors act on the matter state. This allows us to decompose the master equation in terms of the measurement basis as a series of equations $P_m\dot{\hat{\rho}}P_n$. For $m = n$, $P_m\dot{\hat{\rho}}P_m = -iP_m\left[\hat{H}_0, \hat{\rho}\right]P_m$, the measurement terms disappear which shows that a state in a single eigenspace is unaffected by observation. On the other hand, for $m \neq n$ the Hamiltonian evolution actively competes against measurement. In general, if $\hat{a}$ does not commute with the Hamiltonian then a projection to a single eigenspace P_m is impossible.

We now define a new type of projector $\mathscr{P}_M = \sum_{m\in M} P_m$, such that $\mathscr{P}_M\mathscr{P}_N = \delta_{M,N}\mathscr{P}_M$ and $\sum_M \mathscr{P}_M = \hat{1}$ where M denotes some arbitrary subspace. The first equation implies that the subspaces can be built from P_m whilst the second and third equation specify that these projectors do not overlap and that they cover the whole Hilbert space. Furthermore, we will also require that $[\mathscr{P}_M, \hat{H}_0] = [\mathscr{P}_M, \hat{a}] = 0$. The second commutator simply follows from the definition of $\mathscr{P}_M$, but the first one is non-trivial. However, if we can show that $\mathscr{P}_M = \sum_{m\in M} |h_m\rangle\langle h_m|$, where $|h_m\rangle$ is an eigenstate of $\hat{H}_0$ then the commutator is guaranteed to be zero. Note that we always have the trivial case where all these conditions are satisfied and that is when there is only one such projector $\mathscr{P}_M = \hat{1}$.

Assuming that it is possible to have non-trivial cases where $\mathscr{P}_M \neq \hat{1}$ we can write the master equation as

$$\mathscr{P}_M\dot{\hat{\rho}}\mathscr{P}_N = -i\left[\hat{H}_0, \mathscr{P}_M\hat{\rho}\mathscr{P}_N\right] + 2\kappa\left[\hat{a}\mathscr{P}_M\hat{\rho}\mathscr{P}_N\hat{a}^\dagger - \frac{1}{2}\left(\hat{a}^\dagger\hat{a}\mathscr{P}_M\hat{\rho}\mathscr{P}_N + \mathscr{P}_M\hat{\rho}\mathscr{P}_N\hat{a}^\dagger\hat{a}\right)\right]. \tag{13}$$

Crucially, thanks to the commutation relations we were able to divide the density matrix in such a way that each submatrix's time evolution depends only on itself. When we partitioned the matrix with P_m the fact that the projectors did not commute with the operators meant that we had terms of the form $P_m[\hat{H}_0, \hat{\rho}]P_n$ which couple many different $P_m\hat{\rho}P_n$ submatrices with each other.

We note that when $M = N$ the equations for $\mathscr{P}_M\hat{\rho}\mathscr{P}_M$ will include subspaces unaffected by measurement, i.e. $P_m\hat{\rho}P_m$. Therefore, parts of the $\mathscr{P}_M\hat{\rho}\mathscr{P}_M$ submatrices will also remain unaffected by measurement. However, the submatrices $\mathscr{P}_M\hat{\rho}\mathscr{P}_N$, for which $M \neq N$, are guaranteed to not contain measurement-free subspaces thanks to the orthogonality of $\mathscr{P}_M$. Therefore, for $M \neq N$ all elements of $\mathscr{P}_M\hat{\rho}\mathscr{P}_N$ will experience a non-zero measurement term whose effect is always dissipative/lossy. Furthermore, these coherence submatrices $\mathscr{P}_M\hat{\rho}\mathscr{P}_N$ are not coupled to any other part of the density matrix and so they can never increase in magnitude; the remaining coherent evolution is unable to counteract the dissipative term without an 'external pump' from other parts of the density matrix. The combined effect is such that all $\mathscr{P}_M\hat{\rho}\mathscr{P}_N$ for which $M \neq N$ will always go to zero.

When all these cross-terms vanish, we are left with a density matrix that is a mixed state of the form $\hat{\rho} = \sum_M \mathscr{P}_M\hat{\rho}\mathscr{P}_M$. Since there are no coherences, $\mathscr{P}_M\hat{\rho}\mathscr{P}_N$, this state contains only classical uncertainty about which subspace, $\mathscr{P}_M$, is occupied - there are no quantum superpositions between different $\mathscr{P}_M$ spaces. Therefore, in a single measurement run we are guaranteed to have a state that lies entirely within a subspace defined by $\mathscr{P}_M$.

Before moving on to a specific example we will briefly discuss the regime of validity of this result. In principle, this should be applicable to any open system that can be described by the master equation in Eq. (12) as the projectors P_m can be constructed for any jump operator. The peculiar form of our operators, namely that $\hat{a} = C(\hat{D} + \hat{B})$, simply allows us to limit our system to just the matter state, but is in general not necessary to obtain the result above. In fact, QND measurements, such as the one seen in the previous section, are another special case where each of the new projectors $\mathscr{P}_M$ is made of a sum of projectors P_m in a single degenerate subspace. Therefore, the existence of these emergent subspaces relies on exactly the same physical approximations as the master equation and is simply one of the properties of Markovian open systems. However, the existence of these trivial cases alone does not justify the introduction of a new set of projectors. Furthermore, the derivation alone does not help us in identifying what systems might have non-trivial subspaces or whether any even exist. Since this result applies to any system described by a master equation which will always exhibit the trivial cases of the identity and QND measurement projectors, it is unclear whether it is in general possible to predict which Hamiltonians might have these non-trivial emergent subspaces.

However, it turns out that such a non-trivial case is indeed possible for our $\hat{H}_0$ and $\hat{a} = C\hat{B}_2$ and we can see the effect in Fig. 2. Whilst the result is general and applicable to any Markovian system, we identified the first non-trivial case only for phase observable measurements in an optical lattice. This is thanks to the fact that the measurement operator is similar in form to the Hamiltonian, but at the same time it does not commute with it (otherwise we would have a QND measurement).

In Fig. 2 we can clearly see how a state that was initially a superposition of a large number of eigenstates of both operators becomes confined to some small subspace that is neither an eigenspace of $\hat{a}$ or $\hat{H}_0$. In this case the projective spaces, $\mathscr{P}_M$,

are defined by the parities (odd or even) of the combined number of atoms in the β_k and $\tilde{\beta}_k$ modes for different momenta $0 < k < \pi/a$ that are distinguishable to $\hat{B}_2$. The explanation requires careful consideration of where the eigenstates of the two operators overlap and is described in Section S3 of the Supplementary Information online.

To understand the physical meaning of these projections we define an operator $\hat{O}$ with eigenspace projectors R_m, which commutes with both $\hat{H}_0$ and $\hat{a}$. Physically this means that $\hat{O}$ is a compatible observable with $\hat{a}$ and corresponds to a quantity conserved by the Hamiltonian. The fact that $\hat{O}$ commutes with the Hamiltonian implies that the projectors can be written as a sum of Hamiltonian eigenstates $R_m = \sum_{h_i = h_m} |h_i\rangle\langle h_i|$ and thus a projector $\mathscr{P}_M = \sum_{m \in M} R_m$ is guaranteed to commute with the Hamiltonian and similarly since $[\hat{O}, \hat{a}] = 0$ $\mathscr{P}_M$ will also commute with $\hat{a}$ as required. Therefore, $\mathscr{P}_M = \sum_{m \in M} R_m = \sum_{m \in M} P_m$ will satisfy all the necessary prerequisites. This is illustrated in Fig. 3.
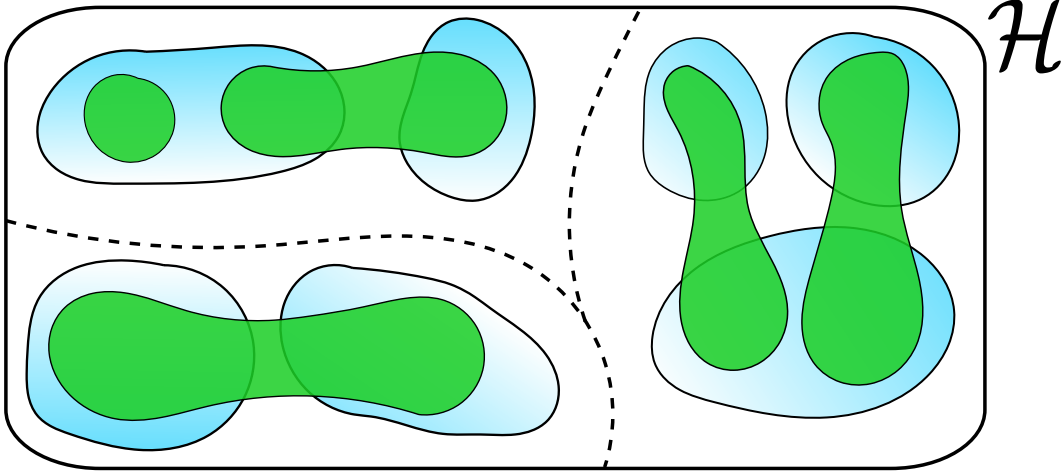

Figure 3. A visual representation of the projection spaces of the measurement. The light blue areas (bottom layer) are R_m, the eigenspaces of $\hat{O}$. The green areas are measurement eigenspaces, P_m, and they overlap non-trivially with the R_m subspaces. The $\mathscr{P}_M$ projection space boundary (dashed line) runs through the Hilbert space, $\mathscr{H}$, where there is no overlap between P_m and R_m.

In the simplest case the projectors $\mathscr{P}_M$ can consist of only single eigenspaces of $\hat{O}$, $\mathscr{P}_M = R_m$. The interpretation is straightforward - measurement projects the system onto a eigenspace of an observable $\hat{O}$ which is a compatible observable with $\hat{a}$ and corresponds to a quantity conserved by the coherent Hamiltonian evolution. However, this may not be possible and we have the more general case when $\mathscr{P}_M = \sum_{m \in M} R_m$. In this case, one can simply think of all $R_{m \in M}$ as degenerate just like eigenstates of the measurement operator, $\hat{a}$, that are degenerate, can form a single eigenspace P_m. However, these subspaces will correspond to different eigenvalues of $\hat{O}$ distinguishing it from conventional projections.

In our case, it is apparent from the form of $\hat{B}_2$ and $\hat{H}_0$ that $\hat{O}_k = \beta_k^\dagger \beta_k + \tilde{\beta}_k^\dagger \tilde{\beta}_k = \hat{n}_k + \hat{n}_{k-\pi/a}$ commutes with both operators for all k. Thus, we can easily construct $\hat{O} = \sum_{\text{RBZ}} g_k \hat{O}_k$ for any arbitrary g_k. Its eigenspaces, R_m, can then be easily constructed and their relationship with P_m and $\mathscr{P}_M$ is illustrated in Fig. 3 whilst the time evolution of $\langle \hat{O}_k \rangle$ for a sample trajectory is shown in Fig. 2(a). These eigenspaces are composed of Fock states in momentum space that have the same number of atoms within each pair of k and $k - \pi/a$ modes. The projectors $\mathscr{P}_M$ consist of many such eigenspaces leading to the case where we can only distinguish between the spaces that have different parities of $\hat{O}_k$.

Experimental considerations

Before concluding this paper, it is worthwhile to consider the experimental difficulties in realising such an experiment. First, we note that there are two recent experiments that have successfully obtained an ultracold gas in an optical lattice coupled to a high-Q cavity[32,33]. The main major concern is photon detector inefficiency. It has been shown[31] that as long as there is a sufficient number of photons detected such that the true instantaneous rate can be reliably estimated it is possible to use detectors with very low efficiencies. Another, possible issue is the sensitivity of the relative angle between the cavity and the probe beams. Generally, the most interesting arrangements, such as the two cases used in this paper, correspond to easily identifiable scattering features such as diffraction maxima and minima, and thus they should be easy to identify and tune. However, it is also possible to obtain identical jump operators with a homodyne detection scheme in which instead of angles, one has to tune the local oscillator phase which might potentially be easier to fine tune in an experiment[13]. Finally, one might also be concerned with possible dephasing due to scattering outside of the cavity. However, cavities used by experiments such as those in Ref.[17,33] have a Purcell factor of ~ 100 and probe-atom detunings in the MHz range. Thus, any scattering outside of

the cavity can be safely neglected[17].

Discussion

In summary we have investigated measurement backaction resulting from coupling light to an ultracold gas's phase-related observables. We demonstrated how this can be used to prepare the Hamiltonian eigenstates even if significant tunnelling is occuring as the measurement can be engineered to not compete with the system's dynamics. Furthermore, we have shown that when the observable of the phase-related quantities does not commute with the Hamiltonian we still project to a specific subspace of the system that is neither an eigenspace of the Hamiltonian or the measurement operator. This is in contrast to quantum Zeno dynamics[49–53] or dissipative state preparation[59]. We showed that this projection is essentially an extension of the measurement postulate to weak measurement on dynamical systems where the competition between the two processes is significant.

Supplementary Information

S1 Suppressing the effective coupling to atomic density

In the main text we showed that $\hat{a} = C(\hat{D} + \hat{B})$, where

$$C = \frac{g_{\text{out}} g_{\text{in}} a_0}{\Delta_a (\Delta_p + i\kappa)}, \tag{S1}$$

$g_{\text{out,in}}$ are the atom-light coupling constants for the outgoing and incoming beams, Δ_a is the detuning between the incoming probe beam and the atomic resonance frequency, Δ_p is the detuning between the incoming probe beam and the outgoing cavity beam, a_0 is the amplitude of the coherent probe beam, and κ is the cavity decay rate. However, we are only interested in the case when $\hat{a} = C\hat{B}$. Therefore, we need to find the conditions under which this is true. For clarity we will consider a 1D lattice, but the results can be applied and generalised to higher dimensions. Central to engineering the $\hat{a}$ operator are the coefficients $J_{m,n}$ given by

$$J_{m,n} = \int w(\mathbf{r} - \mathbf{r}_m) u_{\text{out}}^*(\mathbf{r}) u_{\text{in}}(\mathbf{r}) w(\mathbf{r} - \mathbf{r}_n) \, d\mathbf{r}, \tag{S2}$$

where $w(\mathbf{r})$ are the Wannier functions of the lowest band, $u_{\text{in,out}}(\mathbf{r})$ are the light mode functions of the incoming and outgoing beams, and $\mathbf{r}$ is the position vector. The operators $\hat{B}$ and $\hat{D}$ depend on the values of $J_{m,m+1}$ and $J_{m,m}$ respectively and are given by

$$\hat{D} = \sum_m^K J_{m,m} \hat{n}_m, \tag{S3}$$

$$\hat{B} = \sum_m^K J_{m,m+1} \left(b_m^\dagger b_{m+1} + b_m b_{m+1}^\dagger \right), \tag{S4}$$

where b_m annihilates an atom at site m, and $\hat{n}_m = b_m^\dagger b_m$ is the number operator at site m. These $J_{m,n}$ coefficients are determined by the convolution of the light mode product, $u_{\text{out}}^*(\mathbf{r}) u_{\text{in}}(\mathbf{r})$ with the relevant Wannier function overlap $w(\mathbf{r} - \mathbf{r}_m) w(\mathbf{r} - \mathbf{r}_n)$. For the $\hat{B}$ operator we calculate the convolution with the nearest neighbour overlap, $W_1(\mathbf{r}) \equiv w(\mathbf{r} - \mathbf{a}/2) w(\mathbf{r} + \mathbf{a}/2)$, where $\mathbf{a}$ is the site separation vector, and for the $\hat{D}$ operator we calculate the convolution with the square of the Wannier function at a single site, $W_0(\mathbf{r}) \equiv w^2(\mathbf{r})$. Therefore, in order to enhance the $\hat{B}$ term we need to maximise the overlap between the light modes and the nearest neighbour Wannier overlap, $W_1(\mathbf{r})$. This can be achieved by concentrating the light between the sites rather than at atom positions.

In order to calculate the $J_{m,n}$ coefficients it is necessary to perform numerical calculations using realistic Wannier functions. However, it is possible to gain some analytic insight into the behaviour of these values by looking at the Fourier transforms of the Wannier function overlaps, $\mathscr{F}[W_{0,1}](\mathbf{k})$. This is because the light mode product, $u_{\text{out}}^*(\mathbf{r}) u_{\text{in}}(\mathbf{r})$, can be in general decomposed into a sum of oscillating exponentials of the form $e^{i\mathbf{k}\cdot\mathbf{r}}$ making the integral in Eq. (S2) a sum of Fourier transforms of $W_{0,1}(\mathbf{r})$.

We consider a setup shown in Fig. S1 and take both the detected and probe beam to be standing waves, $u_{\text{in,out}}(\mathbf{r}) = \cos(\mathbf{k}_{\text{in,out}} \cdot \mathbf{r} + \varphi_{\text{in,out}})$, where $\mathbf{k}$ is the wavevector of the beam and φ is a constant phase shift. This gives the following expressions for the $\hat{D}$ and $\hat{B}$ operators

$$\hat{D} = \frac{1}{2} [\mathscr{F}[W_0](k_-) \sum_m \hat{n}_m \cos(k_- x_m + \varphi_-) + \mathscr{F}[W_0](k_+) \sum_m \hat{n}_m \cos(k_+ x_m + \varphi_+)], \tag{S5}$$

$$\hat{B} = \frac{1}{2} [\mathscr{F}[W_1](k_-) \sum_m \hat{p}_m \cos(k_- x_m + \frac{k_- a}{2} + \varphi_-) + \mathscr{F}[W_1](k_+) \sum_m \hat{p}_m \cos(k_+ x_m + \frac{k_+ a}{2} + \varphi_+)], \tag{S6}$$

where $x_m = ma$, $k_\pm = k_{\text{in},x} \pm k_{\text{out},x}$, $k_{(\text{in,out})x} = k_{\text{in,out}} \sin(\theta_{\text{in,out}})$, $\hat{p}_m = b_m^\dagger b_{m+1} + b_m b_{m+1}^\dagger$, and $\varphi_\pm = \varphi_{\text{in}} \pm \varphi_{\text{out}}$. The key result is that the $\hat{B}$ operator is phase shifted by $k_\pm d/2$ with respect to the $\hat{D}$ operator since it depends on the amplitude of light in between the lattice sites and not at the positions of the atoms, allowing to decouple them at specific angles.
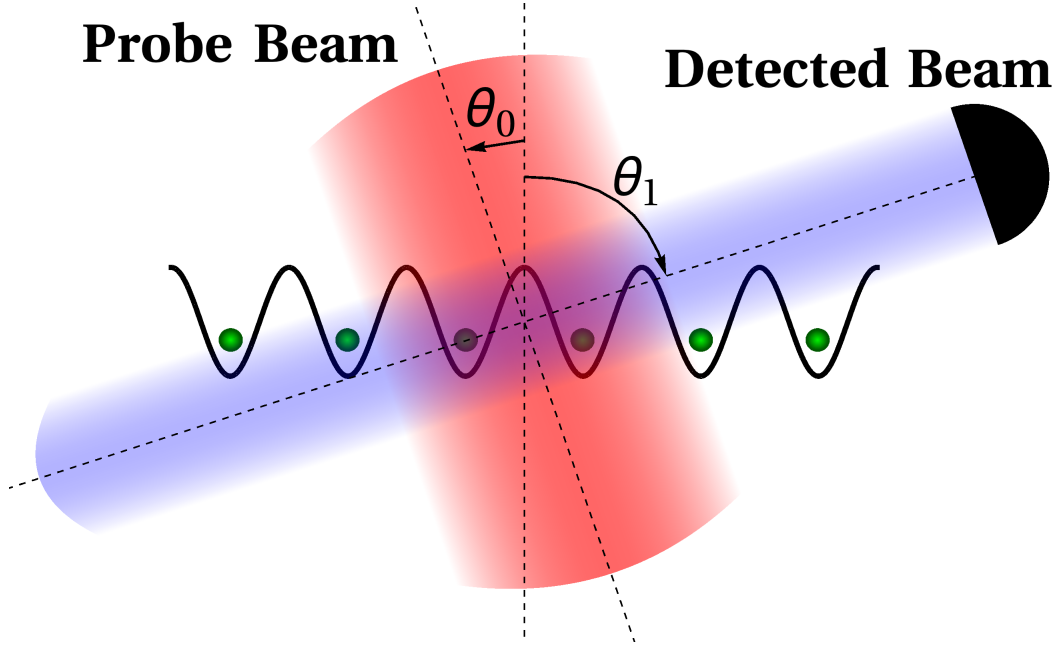

Figure S1. Setup. Atoms in an optical lattice are illuminated by a probe beam. The light scatters in free space or into a cavity and is measured by a detector.

Firstly, we will use this result to show how one can obtain the uniform pattern for which $\hat{B} = \hat{B}_1$, where

$$\hat{B}_1 = \sum_m^K J_1 \left(b_m^\dagger b_{m+1} + b_m b_{m+1}^\dagger \right), \tag{S7}$$

i.e. $J_{m,m+1} = J_1$ This can be achieved by crossing the light modes such that $\theta_{\text{in}} = -\theta_{\text{out}}$ and $k_{\text{in},x} = k_{\text{out},x} = \pi/a$ and choosing the light mode phases such that $\varphi_+ = \pi$. In order to make the $\hat{B}$ contribution to light scattering dominant we need to set $\hat{D} = 0$ which from Eq. (S5) we see is possible if $\varphi_- = \arccos[\mathscr{F}[W_0](2\pi/a)/\mathscr{F}[W_0](0)]/2$. This arrangement of light modes maximizes the interference signal, $\hat{B}$, by suppressing the density signal, $\hat{D}$, via interference compensating for the spreading of the Wannier functions and leads to the parameter value $J_1 = \mathscr{F}[W_1](2\pi/a)/2$. The light mode patterns are illustrated in the main text in Fig. 1(a).

Secondly, we show that we can have a spatially varying pattern for which $\hat{B} = \hat{B}_2$, where

$$\hat{B}_2 = \sum_m^K (-1)^m J_2 \left(b_m^\dagger b_{m+1} + b_m b_{m+1}^\dagger \right). \tag{S8}$$

We consider an arrangement where the beams are arranged such that $k_{\text{in},x} = 0$ and $k_{\text{out},x} = \pi/a$ which gives the following expressions for the density and interference terms

$$\hat{D} = \mathscr{F}[W_0](\pi/a) \sum_m (-1)^m \hat{n}_m \cos(\varphi_{\text{in}}) \cos(\varphi_{\text{out}})$$

$$\hat{B} = -\mathscr{F}[W_1](\pi/a) \sum_m (-1)^m \hat{p}_m \cos(\varphi_{\text{in}}) \sin(\varphi_{\text{out}}). \tag{S9}$$

It is clear that for $\varphi_{\text{out}} = \pm\pi/2$, $\hat{D} = 0$, which is intuitive as this places the lattice sites at the nodes of the mode $u_{\text{out}}(\mathbf{r})$ and yields the parameter value $J_2 = -\mathscr{F}[W_1](\pi/a) \cos(\varphi_{\text{in}})$. This is a diffraction minimum as the light amplitude is zero, $\langle \hat{B} \rangle = 0$,

because contributions from alternating inter-site regions interfere destructively. However, the intensity $\langle \hat{a}^\dagger \hat{a} \rangle = |C|^2 \langle \hat{B}^2 \rangle$ is proportional to the variance of $\hat{B}$ and is non-zero. The light mode patterns are illustrated in the main text in Fig. 1(b).

S2 Finding the measurement projection subspaces

The main text defines the projectors $\mathscr{P}_M = \sum_{m \in M} P_m$, where P_m are the projectors onto the $\hat{a}$ eigenspaces, such that $\sum_M \mathscr{P}_M = \hat{1}$, $\mathscr{P}_M \mathscr{P}_N = \delta_{M,N} \mathscr{P}_M$, $[\mathscr{P}_M, \hat{H}_0] = 0$, and $[\mathscr{P}_M, \hat{a}] = 0$. To find $\mathscr{P}_M$ we need to identify the subspaces M which satisfy the following relation $\sum_{m \in M} P_m = \sum_{m \in M} |h_m\rangle\langle h_m|$, where $|h_m\rangle$ are the eigenstates of $\hat{H}_0$. This can be done iteratively by (i) selecting some P_m, (ii) identifying the $|h_m\rangle$ which overlap with this subspace, (iii) identifying any other P_m which also overlap with these $|h_m\rangle$ from step (ii). We repeat (ii)-(iii) for all the P_m found in (iii) until we have identified all the subspaces P_m linked in this way and they will form one of our $\mathscr{P}_M$ projectors. If $\mathscr{P}_M \neq 1$ then there will be other subspaces P_m which we have not included so far and thus we repeat this procedure on the unused projectors until we identify all $\mathscr{P}_M$. Computationally this can be straightforwardly solved with some basic algorithm that can compute the connected components of a graph.

The above procedure, whilst mathematically correct and always guarantees to generate the projectors $\mathscr{P}_M$, is very unintuitive and gives poor insight into the nature or physical meaning of $\mathscr{P}_M$. In order to get a better understanding of these subspaces we will use another result from the main text. We showed that for an operator $\hat{O}$ with eigenspace projectors R_m for which $[\hat{O}, \hat{H}_0] = 0$, and $[\hat{O}, \hat{a}] = 0$, then we can write the subspace projectors as $\mathscr{P}_M = \sum_{m \in M} R_m = \sum_{m \in M} P_m$.

We are interested in identifying these subspaces for the operator $\hat{B}_2$ given by

$$
\begin{aligned}
\hat{B}_2 &= \sum_m^K (-1)^m J_2 \left(b_m^\dagger b_{m+1} + b_m b_{m+1}^\dagger \right) \\
&= 2iJ_2 \sum_k c_k^\dagger c_{k-\pi/a} \sin(ka).
\end{aligned}
\tag{S10}
$$

We have identified that for $\hat{B}_2$, an operator $\hat{O}$ that commutes with both the measurement operator and the Hamiltonian is given by $\hat{O} = \sum_{\text{RBZ}} g_k \hat{O}_k$, where $\hat{O}_k = \hat{n}_k + \hat{n}_{k-\pi/a}$, for any arbitrary constants g_k. The subspaces R_m of this operator simply consist of momentum space Fock states that have the same number of atoms in each $(k, k - \pi/a)$ pair of momenta. However, it turns out that the $\mathscr{P}_M$ consist of multiple such subspaces complicating the picture.

Firstly, since $\hat{B}_2$ contains $\sin(ka)$ coefficients atoms in different k modes that have the same $\sin(ka)$ value are indistinguishable to the measurement and will lie in the same P_m eigenspaces. This will happen for the pairs $(k, \pi/a - k)$. Therefore, the R_m spaces that have the same $\hat{O}_k + \hat{O}_{\pi/a-k}$ eigenvalues must belong to the same $\mathscr{P}_M$.

Secondly, if we re-write these operators in terms of the β_k and $\tilde{\beta}_k$ modes we get

$$
\hat{B}_2 = 2J_2 \sum_{\text{RBZ}} \sin(ka) \left(\beta_k^\dagger \beta_k - \tilde{\beta}_k^\dagger \tilde{\beta}_k \right),
\tag{S11}
$$

$$
\hat{O} = \sum_{\text{RBZ}} g_k \left(\beta_k^\dagger \beta_k + \tilde{\beta}_k^\dagger \tilde{\beta}_k \right),
\tag{S12}
$$

and so it's not hard to see that $\hat{B}_{2,k} = (\beta_k^\dagger \beta_k - \tilde{\beta}_k^\dagger \tilde{\beta}_k)$ will have the same eigenvalues for different values of $\hat{O}_k = \beta_k^\dagger \beta_k + \tilde{\beta}_k^\dagger \tilde{\beta}_k$. Specifically, if a given subspace R_m corresponds to the eigenvalue O_k of $\hat{O}_k$ then the possible values of $B_{2,k}$ will be $\{-O_k, -O_k + 2, ..., O_k - 2, O_k\}$. Thus, we can see that all R_m with even values of O_k will share $B_{2,k}$ eigenvalues and thus they will overlap with the same P_m subspaces. The same is true for odd values of O_k. However, R_m with an even value of O_k will never have the same value of $B_{2,k}$ as a subspace with an odd value of O_k. Therefore, a single $\mathscr{P}_M$ will contain all R_m that have the same parities of O_k for all k, e.g. if it includes the R_m with $O_k = 6$, it will also include the R_m for which $O_k = 0, 2, 4, 6, ..., N$, where N is the total number of atoms.

Finally, the $k = \pi/a$ mode is special, because $\sin(\pi) = 0$ which means that $B_{2,k=\pi/a} = 0$ always. This in turn implies that all possible values of $O_{\pi/a}$ are degenerate to the measurement. Therefore, we exclude this mode when matching the parities of the other modes.

To illustrate the above let us consider a specific example. Let us consider two atoms, $N = 2$, on eight sites $M = 8$. This configuration has eight momentum modes $ka = \{-\frac{3\pi}{4}, -\frac{\pi}{2}, -\frac{\pi}{4}, 0, \frac{\pi}{4}, \frac{\pi}{2}, \frac{3\pi}{4}, \pi\}$ and so the RBZ has only four modes RBZ $:= \{\frac{\pi}{4}, \frac{\pi}{2}, \frac{3\pi}{4}, \pi\}$. There are 10 different ways of splitting two atoms into these four modes and thus we have 10 different $R_m = \{O_{\pi/4a}, O_{\pi/2a}, O_{3\pi/4a}, O_{\pi/a}\}$ eigenspaces of $\hat{O}$ and they are shown in Table S1. In the third column we have also listed the eigenvalues of the $\hat{B}_2$ eigenstates that lie within the given R_m.

m	R_m	Possible values of $B_{\min}$
0	$\{2,0,0,0\}$	$-\sqrt{2}, 0, \sqrt{2}$
1	$\{1,1,0,0\}$	$-\frac{1+\sqrt{2}}{\sqrt{2}}, -\frac{1-\sqrt{2}}{\sqrt{2}}, \frac{1-\sqrt{2}}{\sqrt{2}}, \frac{1+\sqrt{2}}{\sqrt{2}}$
2	$\{1,0,1,0\}$	$-\sqrt{2}, 0, \sqrt{2}$
3	$\{1,0,0,1\}$	$-\frac{1}{\sqrt{2}}, \frac{1}{\sqrt{2}}$
4	$\{0,2,0,0\}$	$-2, 0, 2$
5	$\{0,1,1,0\}$	$-\frac{1+\sqrt{2}}{\sqrt{2}}, -\frac{1-\sqrt{2}}{\sqrt{2}}, \frac{1-\sqrt{2}}{\sqrt{2}}, \frac{1+\sqrt{2}}{\sqrt{2}}$
6	$\{0,1,0,1\}$	$-1, 1$
7	$\{0,0,2,0\}$	$-\sqrt{2}, 0, \sqrt{2}$
8	$\{0,0,1,1\}$	$-\frac{1}{\sqrt{2}}, \frac{1}{\sqrt{2}}$
9	$\{0,0,0,2\}$	0

Table S1. A list of all R_m eigenspaces for $N = 2$ atoms at $M = 8$ sites. The third column displays the eigenvalues of all the eigenstates of $\hat{B}_2$ that lie in the given R_m.

We note that $ka = \pi/4$ will be degenerate with $ka = 3\pi/4$ since $\sin(ka)$ is the same for both. Therefore, we already know that we can combine (R_0, R_2, R_7), (R_1, R_5), and (R_3, R_8), because those combinations have the same $O_{\pi/4a} + O_{3\pi/4a}$ values. This is very clear in the table as these subspaces span exactly the same values of B_2.

Now we have to match the parities. Subspaces that have the same parity combination for the pair $(O_{\pi/4a} + O_{3\pi/4a}, O_{\pi/2a})$ will be degenerate in $\mathscr{P}_M$. Note that we excluded $O_{\pi/a}$, because as we discussed earlier they are all degenerate due to $\sin(\pi) = 0$. Therefore, the (even,even) subspace will include $(R_0, R_2, R_4, R_7, R_9)$, the (odd,even) will contain (R_3, R_8), the (even, odd) will contain (R_6) only, and the (odd, odd) contains (R_1, R_5). These overlaps should be evident from the table as we can see that these combinations combine all R_m that contain any eigenstates of $\hat{B}_2$ with the same eigenvalues.

Therefore, we have end up with four distinct $\mathscr{P}_M$ subspaces

$$\mathscr{P}_{\text{even,even}} = R_0 + R_2 + R_4 + R_7 + R_9$$
$$\mathscr{P}_{\text{odd,even}} = R_3 + R_8$$
$$\mathscr{P}_{\text{even,odd}} = R_6$$
$$\mathscr{P}_{\text{odd,odd}} = R_1 + R_5.$$

At this point it should be clear that these projectors satisfy all our requirement. The conditions $\sum_M \mathscr{P}_M = 1$ and $\mathscr{P}_M \mathscr{P}_N = \delta_{M,N} \mathscr{P}_M$ should be evident from the form above. The commutator requirements are also easily satisfied since the subspaces R_m are of an operator that commutes with both the Hamiltonian and the measurement operator. And finally, one can also verify using the table that all of these projectors are built from complete subspaces of $\hat{B}_2$ (i.e. each subspace P_m belongs to only one $\mathscr{P}_M$) and thus $\mathscr{P}_M = \sum_{m \in M} P_m$.

References

1. Lewenstein, M. *et al.* Ultracold atomic gases in optical lattices: mimicking condensed matter physics and beyond. *Advances in Physics* **56**, 243–379 (2007).

2. Bloch, I., Dalibard, J. & Zwerger, W. Many-body physics with ultracold gases. *Reviews of Modern Physics* **80**, 885 (2008).

3. Mekhov, I. B. & Ritsch, H. Quantum optics with ultracold quantum gases: towards the full quantum regime of the light–matter interaction. *Journal of Physics B: Atomic, Molecular and Optical Physics* **45**, 102001 (2012).

4. Ritsch, H., Domokos, P., Brennecke, F. & Esslinger, T. Cold atoms in cavity-generated dynamical optical potentials. *Reviews of Modern Physics* **85**, 553 (2013).

5. Eckert, K. *et al.* Quantum non-demolition detection of strongly correlated systems. *Nature Physics* **4**, 50–54 (2008).

6. Roscilde, T. *et al.* Quantum polarization spectroscopy of correlations in attractive fermionic gases. *New Journal of Physics* **11**, 055041 (2009).

7. Mekhov, I. B. & Ritsch, H. Quantum optics with quantum gases: Controlled state reduction by designed light scattering. *Physical Review A* **80**, 013604 (2009).

8. De Chiara, G., Romero-Isart, O. & Sanpera, A. Probing magnetic order in ultracold lattice gases. *Physical Review A* **83**, 021604 (2011).

9. Mekhov, I. B. Quantum non-demolition detection of polar molecule complexes: dimers, trimers, tetramers. *Laser Physics* **23**, 015501 (2013).

10. Hauke, P., Sewell, R. J., Mitchell, M. W. & Lewenstein, M. Quantum control of spin correlations in ultracold lattice gases. *Physical Review A* **87**, 021601 (2013).

11. Rogers, B., Paternostro, M., Sherson, J. F. & De Chiara, G. Characterization of bose-hubbard models with quantum nondemolition measurements. *Physical Review A* **90**, 043618 (2014).

12. Elliott, T. J., Kozlowski, W., Caballero-Benitez, S. F. & Mekhov, I. B. Multipartite entangled spatial modes of ultracold atoms generated and controlled by quantum measurement. *Physical review letters* **114**, 113604 (2015).

13. Kozlowski, W., Caballero-Benitez, S. F. & Mekhov, I. B. Probing matter-field and atom-number correlations in optical lattices by global nondestructive addressing. *Physical Review A* **92**, 013613 (2015).

14. Elliott, T. J., Mazzucchi, G., Kozlowski, W., Caballero-Benitez, S. F. & Mekhov, I. B. Probing and manipulating fermionic and bosonic quantum gases with quantum light. *Atoms* **3**, 392–406 (2015).

15. Moore, M. G., Zobay, O. & Meystre, P. Quantum optics of a bose-einstein condensate coupled to a quantized light field. *Physical Review A* **60**, 1491 (1999).

16. Chen, W. & Meystre, P. Cavity qed characterization of many-body atomic states in double-well potentials: Role of dissipation. *Physical Review A* **79**, 043801 (2009).

17. Baumann, K., Guerlin, C., Brennecke, F. & Esslinger, T. Dicke quantum phase transition with a superfluid gas in an optical cavity. *Nature* **464**, 1301–1306 (2010).

18. Wolke, M., Klinner, J., Keßler, H. & Hemmerich, A. Cavity cooling below the recoil limit. *Science* **337**, 75–78 (2012).

19. Schmidt, D., Tomczyk, H., Slama, S. & Zimmermann, C. Dynamical instability of a bose-einstein condensate in an optical ring resonator. *Physical review letters* **112**, 115302 (2014).

20. Caballero-Benitez, S. F. & Mekhov, I. B. Quantum optical lattices for emergent many-body phases of ultracold atoms. *Physical review letters* **115**, 243604 (2015).

21. Caballero-Benitez, S. F. & Mekhov, I. B. Quantum properties of light scattered from structured many-body phases of ultracold atoms in quantum optical lattices. *New Journal of Physics* **17**, 123023 (2015).

22. Mazzucchi, G., Caballero-Benitez, S. F. & Mekhov, I. B. Quantum measurement-induced antiferromagnetic order and density modulations in ultracold fermi gases in optical lattices. *Scientific reports* **6**, 31196 (2016).

23. Caballero-Benitez, S. F., Mazzucchi, G. & Mekhov, I. B. Quantum simulators based on the global collective light-matter interaction. *Phys. Rev. A* **93**, 063632 (2016). URL http://link.aps.org/doi/10.1103/PhysRevA.93.063632.

24. Lee, M. D. & Ruostekoski, J. Classical stochastic measurement trajectories: Bosonic atomic gases in an optical cavity and quantum measurement backaction. *Physical Review A* **90**, 023628 (2014).

25. Blattmann, R. & Mølmer, K. Conditioned quantum dynamics in a 1d lattice system. *Physical Review A* **93**, 052113 (2016).

26. Ashida, Y. & Ueda, M. Diffraction-unlimited position measurement of ultracold atoms in an optical lattice. *Physical review letters* **115**, 095301 (2015).

27. Ashida, Y. & Ueda, M. Multi-particle quantum dynamics under continuous observation. *arXiv preprint arXiv:1510.04001* (2015).

28. Ashida, Y., Furukawa, S. & Ueda, M. Quantum critical behavior influenced by measurement backaction in ultracold gases. *Physical Review A* **94**, 053615 (2016).

29. Mazzucchi, G., Kozlowski, W., Caballero-Benitez, S. F., Elliott, T. J. & Mekhov, I. B. Quantum measurement-induced dynamics of many-body ultracold bosonic and fermionic systems in optical lattices. *Physical Review A* **93**, 023632 (2016).

30. Kozlowski, W., Caballero-Benitez, S. F. & Mekhov, I. B. Non-hermitian dynamics in the quantum zeno limit. *Physical Review A* **94**, 012123 (2016).

31. Mazzucchi, G., Kozlowski, W., Caballero-Benitez, S. F. & Mekhov, I. B. Collective dynamics of multimode bosonic systems induced by weak quantum measurement. *New Journal of Physics* **18**, 073017 (2016). URL http://stacks.iop.org/1367-2630/18/i=7/a=073017.

32. Klinder, J., Keßler, H., Bakhtiari, M. R., Thorwart, M. & Hemmerich, A. Observation of a superradiant mott insulator in the dicke-hubbard model. *Physical review letters* **115**, 230403 (2015).

33. Landig, R. *et al.* Quantum phases from competing short-and long-range interactions in an optical lattice. *Nature* **532**, 476–479 (2016).

34. Mekhov, I. B. & Ritsch, H. Quantum optics with quantum gases. *Laser physics* **19**, 610–615 (2009).

35. Caballero-Benitez, S. F. & Mekhov, I. B. Bond order via light-induced synthetic many-body interactions of ultracold atoms in optical lattices. *New Journal of Physics* **18**, 113010 (2016).

36. Cirac, J. I., Gardiner, C. W., Naraschewski, M. & Zoller, P. Continuous observation of interference fringes from bose condensates. *Physical Review A* **54**, R3714 (1996).

37. Castin, Y. & Dalibard, J. Relative phase of two bose-einstein condensates. *Physical Review A* **55**, 4330 (1997).

38. Ruostekoski, J. & Walls, D. F. Nondestructive optical measurement of relative phase between two bose-einstein condensates. *Physical Review A* **56**, 2996 (1997).

39. Ruostekoski, J., Collett, M. J., Graham, R. & Walls, D. F. Macroscopic superpositions of bose-einstein condensates. *Physical Review A* **57**, 511 (1998).

40. Rist, S. & Morigi, G. Homodyne detection of matter-wave fields. *Physical Review A* **85**, 053635 (2012).

41. Hood, C., Chapman, M., Lynn, T. & Kimble, H. Real-time cavity qed with single atoms. *Physical review letters* **80**, 4157 (1998).

42. Murch, K., Weber, S., Macklin, C. & Siddiqi, I. Observing single quantum trajectories of a superconducting quantum bit. *Nature* **502**, 211–214 (2013).

43. Roch, N. *et al.* Observation of measurement-induced entanglement and quantum trajectories of remote superconducting qubits. *Physical review letters* **112**, 170501 (2014).

44. Mekhov, I. B. & Ritsch, H. Quantum optical measurements in ultracold gases: Macroscopic bose-einstein condensates. *Laser physics* **20**, 694–699 (2010).

45. Mekhov, I. B. & Ritsch, H. Atom state evolution and collapse in ultracold gases during light scattering into a cavity. *Laser Physics* **21**, 1486–1490 (2011).

46. Douglas, J. S. & Burnett, K. Scattering-induced spatial superpositions in multiparticle localization. *Physical Review A* **86**, 052120 (2012).

47. Douglas, J. S. & Burnett, K. Scattering distributions in the presence of measurement backaction. *Journal of Physics B: Atomic, Molecular and Optical Physics* **46**, 205301 (2013).

48. Pedersen, M. K., Sørensen, J. J. W., Tichy, M. C. & Sherson, J. F. Many-body state engineering using measurements and fixed unitary dynamics. *New Journal of Physics* **16**, 113038 (2014).

49. Misra, B. & Sudarshan, E. C. G. The zeno's paradox in quantum theory. *Journal of Mathematical Physics* **18**, 756–763 (1977).

50. Facchi, P. & Pascazio, S. Quantum zeno dynamics: mathematical and physical aspects. *Journal of Physics A: Mathematical and Theoretical* **41**, 493001 (2008).

51. Raimond, J. M. *et al.* Phase Space Tweezers for Tailoring Cavity Fields by Quantum Zeno Dynamics. *Phys. Rev. Lett.* **105**, 213601 (2010).

52. Raimond, J. M. *et al.* Quantum Zeno dynamics of a field in a cavity. *Phys. Rev. A* **86**, 032120 (2012).

53. Signoles, A. *et al.* Confined quantum zeno dynamics of a watched atomic arrow. *Nat. Phys.* **10**, 715–719 (2014).

54. Bux, S. *et al.* Control of matter-wave superradiance with a high-finesse ring cavity. *Physical Review A* **87**, 023607 (2013).

55. Keßler, H., Klinder, J., Wolke, M. & Hemmerich, A. Steering matter wave superradiance with an ultranarrow-band optical cavity. *Physical review letters* **113**, 070404 (2014).

56. Landig, R., Brennecke, F., Mottl, R., Donner, T. & Esslinger, T. Measuring the dynamic structure factor of a quantum gas undergoing a structural phase transition. *Nature communications* **6** (2015).

57. Einstein, A., Podolsky, B. & Rosen, N. Can quantum-mechanical description of physical reality be considered complete? *Physical review* **47**, 777 (1935).

58. Brune, M., Haroche, S., Raimond, J. M., Davidovich, L. & Zagury, N. Manipulation of photons in a cavity by dispersive atom-field coupling: Quantum-nondemolition measurements and generation of "schrödinger cat" states. *Physical Review A* **45**, 5193 (1992).

59. Diehl, S. *et al.* Quantum states and phases in driven open quantum systems with cold atoms. *Nat. Phys.* **4**, 878–883 (2008).

60. Kessler, E. M. *et al.* Dissipative phase transition in a central spin system. *Physical Review A* **86**, 012116 (2012).

Acknowledgements

Author contributions statement

W.K. is the lead author and performed the analysis and numerical simulations. S.F.C.-B. and I.B.M. supervised the work. All authors generated ideas for this paper and discussed the text at all stages.

Competing financial interests

The authors declare no competing financial interests.